ACADEMIC PRESS

Available online at www.sciencedirect.com
SCIENCE DIRECT®

Icarus 164 (2003) 79–95

ICARUS

www.elsevier.com/locate/icarus

Cerberus Fossae, Elysium, Mars: a source for lava and water

J.B. Plescia

US Geological Survey, 2255 N. Gemini Drive, Flagstaff, AZ 86001, USA

Received 4 September 2002; revised 24 March 2003

Abstract

Cerberus Fossae, a long fracture system in the southeastern part of Elysium, has acted as a conduit for the release of both lava and water onto the surface. The southeastern portion of the fracture system localized volcanic vents having varying morphology. In addition, low shields occur elsewhere on the Cerberus plains. Three locations where the release of water has occurred have been identified along the northwest (Athabasca and Grjota' Vallis) and southeast (Rahway Vallis) portions of the fossae. Water was released both catastrophically and noncatastrophically from these locations. A fluvial system that extends more than 2500 km has formed beginning at the lower flank of the Elysium rise across the Cerberus plains and out through Marte Vallis into Amazonis Planitia. The timing of the events is Late Amazonian.

1. Introduction

The Cerberus plains are a widespread, level, young surface in southern Elysium extending from approximately 5° S to 10° N and from 175° W to 220° W (Fig. 1). They are the youngest large-scale unit (Tanaka, 1986; Greeley and Guest, 1987) and the youngest major volcanic surface on Mars. Cutting across these plains, and the intervening knobby terrain, are the west–northwest-trending fractures of Cerberus Fossae. The fractures of Cerberus Fossae have acted as conduits for the release of water and lava onto the surface relatively recently in martian geologic history.

The origin of the Cerberus plains material was the subject of some debate on the basis of Viking images with both fluvial (Tanaka et al., 1992; Scott and Chapman, 1995) and volcanic origins (Plescia, 1990) being proposed. The morphology of the surface, as seen in MOC images (McEwen et al., 1998; McEwen, 1999; Keszthelyi et al., 2000) and illustrated by MOLA topography indicates that the present plains surface is volcanic in origin. Although the present upper surface is volcanic, the morphology of the underlying unit clearly documents an earlier widespread fluvial event that carved extensive channel systems (Fig. 2).

Previous studies of the area have suggested the source for both the water and the volcanics to be the Cerberus Fossae, but Viking images did not have sufficient resolution (typically the best resolution was tens of meters) and Viking-era topography was too coarse (1 km contour interval) to identify sources. Flow fronts and albedo patterns around obstacles observed in Viking images provided a general flow direction for the lavas, but a specific source could not be identified. Exposures of the older channeled surfaces observed in Viking images in scattered locations, again provided local indications of water flow direction, but no information on the source region. Thus, it was impossible to define the source region or understand the possible relation between the fluvial and volcanic episodes based solely on Viking data. MOLA and MOC data allow a much better understanding of the volcanic and fluvial history of the region because the details the surface morphology can be observed and small-scale topographic features can be resolved over large distances. Burr et al. (2002b) have already discussed Athabasca Vallis whose source lies along the northwestern end of Cerberus Fossae. Burr et al. (2002a) identified a second source and channel system from the northwestern strand of Cerberus Fossae which flows north and east (referred to here as Grjota' Vallis) and a valley system south of Orcus Patera (referred to here as Rahway Vallis).

Data are presented here illustrating the location and morphology of volcanic sources along the Cerberus Fossae and elsewhere on the Cerberus plains. Building on the obser-

E-mail address: jplescia@usgs.gov.

0019-1035/03/$ – see front matter
doi:10.1016/S0019-1035(03)00139-8

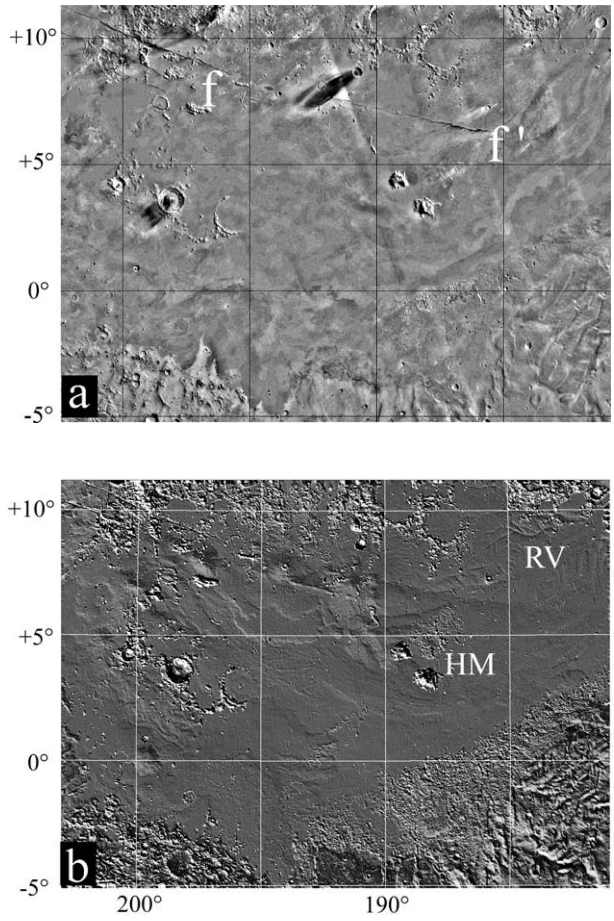

Fig. 1. Cerberus plains and Cerberus Fossae. (a) Viking based mosaic of the area. Resolution 1 km/pixel. The extend of the linear fissure vent is between f and f'. (b) Shaded relief map of the Cerberus plains created using MOLA data, shading is from the south. RV: Rahway Vallis, HB: Hibes Montes.

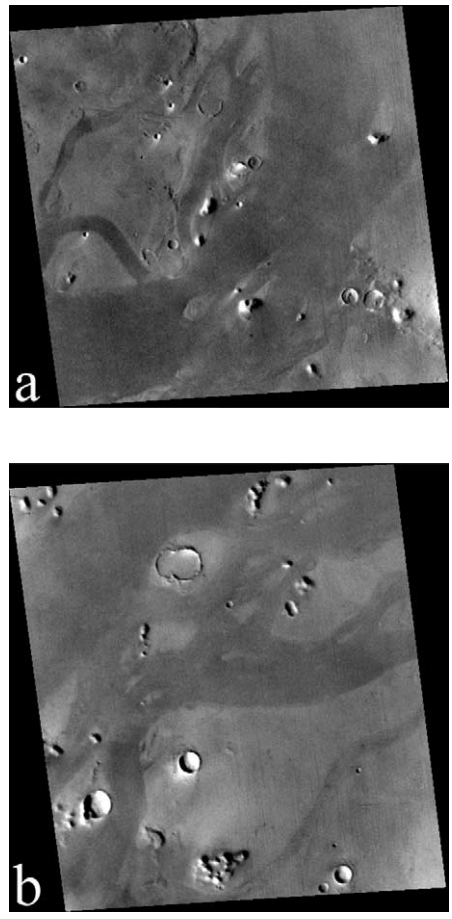

Fig. 2. Marte Vallis showing darker lava-filled channels and lighter older plains. (a) MOC low-resolution image E05-00192, centered at 12.42° N, 177.63° W, resolution 249.89 m/pixel, scene width 121 km. (b) MOC low-resolution image M08-01239, centered at 10.47° N, 179.42° W, resolution 246.59 m/pixel, scene width 119 km.

vations of Burr et al. (2002a, 2002b), data are presented to describe Athabasca Vallis, a second fluvial source north of Athabasca Vallis (Grjota' Vallis), and the valley network at the southeastern end of the Fossae (Rahway Vallis). In order to examine the nature of Cerberus Fossae and identify volcanic and fluvial vents, MOLA data were processed to produce digital elevation models and shaded relief maps with a grid spacing of 500 m. ArcView was used to process the data.

2. Cerberus region

Cerberus Fossae is an extensive fracture system in southern Elysium having variable morphology and age. Fractures extend from about 6.2° N, 185° W to 12° N, 206° W (Fig. 1), a distance of more than 1200 km, with an average orientation of N 80° W in the southeast and N 70° W in the northwest. Individual en echelon segments have slightly more westerly trends than the overall structure. Fracture widths range from tens of meters to over a kilometer; some fractures, however, are too narrow to be resolved even at the resolution of MOC images. Most of the fracture segments have blunt amphitheater terminations.

The interior morphology of the fractures consists of a steep, layered upper slope, presumably consisting of exposed bedrock. Below this is a gentler slope presumably composed of talus. The floor of the fractures is covered with loose material shed off the walls and is partly covered with dunes. Locally, blocks of the wall rock are observed to have slumped into the fractures (e.g., MOC images M07-01049, M12-00756, E05-00598). Fracture morphology appears to be partly controlled by the unit within which the fractures occur and may reflect the strength of the unit. For example, on the volcanic plains the fossae are composed of simple, locally en echelon fractures. In the knobby terrain (near 10° N, 200° W), the fossae are wider (2000 m) and deeper. In addition to the principal structure, many minor fractures and lineaments occur across a wide zone parallel to the main fracture. Cerberus Fossae itself has a subtle topographic expression extending across the young lavas that fill Marte Vallis southeast beyond the zone of surface fracturing (Fig. 1). MOLA topography indicates the feature is a slope break,

separating a north-dipping surface south of the lineament from a horizontal one to the north. The morphology and lateral extent of the Cerberus Fossae indicates it is a major crustal structure.

The Cerberus plains are virtually flat, varying in elevation by only a few hundred meters. For example, the elevation at 178° W is −3 km, whereas at 162.5° W it is −2.8 km, a change of only 200 m across 920 km indicating a regional slopes of the order 0.01°. Such low regional slopes do not necessarily imply the surface is smooth on a smaller scale. Earth-based 12.6 cm Arecibo radar data (Harmon et al., 1999) indicate the Cerberus plains are very rough, showing the plains are among the roughest surfaces observed with radar on Mars.

MOLA data show that the smooth plains of the Cerberus region are not all of the same age or the result of a single episode or style of volcanism as suggested by Plescia (1990). He interpreted all of the smooth materials observed in Viking images, including patches of the plains that embay the knobby terrain to the north, as being part of a single unit composed of flood basalt. MOC images and particularly the MOLA data show that the Cerberus plains are of at least two different ages (based on superposition relations and crater frequencies) and have different morphologies. The southern part of the region, extending from 5° N, 195° W southward around Hibes Montes and into Marte Vallis, is the younger area. The plains to the north, near 7° N, 195° W, are older with more craters and local valley networks (Fig. 1) and do not exhibit the obvious volcanic morphology (e.g., flow fronts and margins) that characterize the plains to the south. Berman and Hartman (2002) suggest, on the basis of crater counts using MOC images, that the region has a complicated, long-lived geologic history extending over hundreds of millions of years to the present.

3. Volcanic sources

Volcanic sources having two morphologies have been identified on the Cerberus plains: linear fissure vents and low shields. Fissure vents result from eruptions along a linear vent producing an elongate topographic high with flows extending away from the vent(s). Low shields are more equant in shape having a localized summit vent(s) and narrow, short flows extending down the flanks. Low shields are different from the fissure vents in that they are characterized by eruptions from a point source, have (in this case) relatively narrow flows extending from the summit region, and are fairly equant in shape (Greeley, 1982). The linear fissure vents have the same trend as Cerberus Fossae. Low shields occur near the fissure vents and elsewhere on the southern part of the Cerberus plains.

On the Cerberus plains, a well-defined linear topographic high trending N 80° W extends about 340 km from 6.54° N, 191.2° W to 8.10° N, 196.62° W (Fig. 1). The central portion is the best developed and extends from 6.713° N, 192.034° W to 7.216° N, 193.858° W, a distance of about 110 km. The ridge, ∼ 20–40-m high and 10-km wide, lies about 40–50 km south of and parallel to Cerberus Fossae probably along a parallel but buried fracture. This feature is interpreted to be a fissure vent with the linear topography resulting from the build up of lava and possibly spatter. The fissure eruption of the Laki Iceland basalt of 1783–1785 (Thorarinsson, 1970; Thordarson and Self, 1993), which may provide an analog, formed a 27-km long fissure vent composed of scoria, spatter and tuff cones arranged in an en echelon pattern. Individual constructs along the Laki fissure rise as much as 120 m and eruption rates were of the order 1.1 to 4.4×10^3 m^3/sec. Fig. 3 shows a group of high-resolution MOC images across the summit of the Cerberus ridge. These images show some vent structure, but few other volcanic landforms such as flows or cones. Possibly the relatively high illumination angle of the MOC images may preclude recognizing subtle features. Alternatively, the absence of observed lava flows may reflect the presence of local pyroclastics or a thick aeolian mantle.

Large lava flows extend to the south of the ridge and southeast across the Cerberus plains (Fig. 1). Many flows appear to originate in the northwest part of the area along the fissure vent. Two obvious flows south of the fissure extend for 140–160 km and 80–100 km and are tens of meters thick. The southern part of the plains, extending to the east of Hibes Montes, is filled with numerous flows many of which are too small to be resolved in the shaded relief maps. Locally, the margins and volcanic characteristics (pressure ridges, lobate margins, etc.) are clearly resolved in the MOC images.

The Cerberus lavas appear to have been erupted from localized sources along Cerberus Fossae. Additional sources, such as fissure vents, may lie in the eastern and southern parts of the plains, but if present they are now buried by younger flows. The low shields may represent sources which produced only limited volumes of lava for a short period of time at low eruption rates, whereas the fissure vents would have produced larger quantities of lava at higher effusion rates. Alternatively, the low shields may have been built at the end of an eruptive cycle as the composition of the lavas changed. Sakimoto et al. (2003) have noted that the steep part of low shields on the Snake River Plain are associated with basalt having vesicles due to volatile loss and large plagioclase laths. These lavas were more viscous than earlier lavas producing steep slopes.

Figure 4 illustrates the low shields as seen in the shaded relief data; morphometric information is listed in Table 1. Three of the vents are in the western Cerberus plains, south of the Cerberus Fossae and approximately at the same longitude (∼ 200° W), west and south of a salient of knobby terrain. The other four have developed along the trend of the fissure. Viking images show albedo/shading patterns that, in retrospect, are suggestive of the presence of the low shields, but again, the morphology of the low shields was

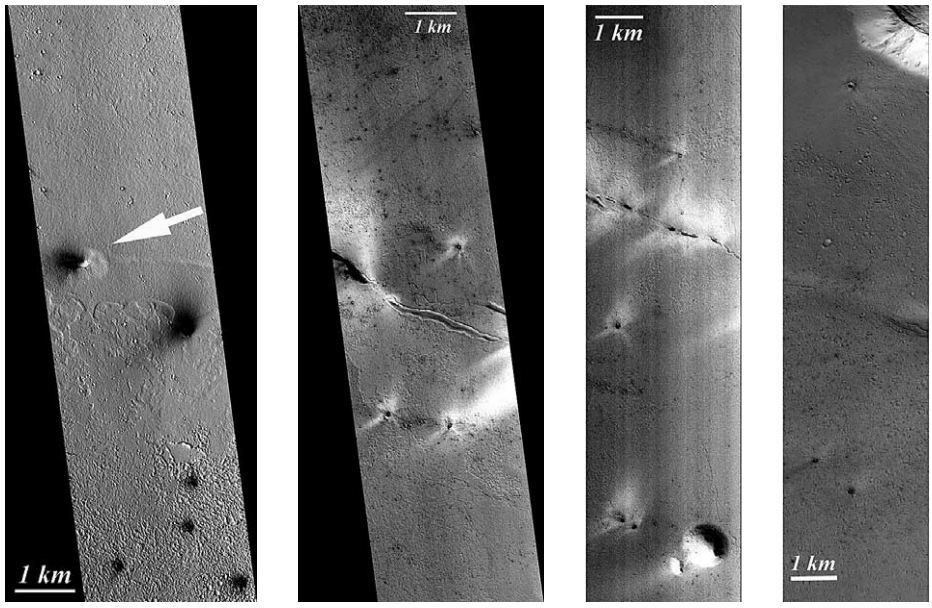

(a) (b) (c) (d)

Fig. 3. MOC images across the summit of the linear volcanic ridge. (a) An elongate vent is observed at the arrow. Small craters have dark ejecta blankets. MOC image E05-01649, 193.27 W, 6.97 N, 5.88 m/pixel. (b) Linear summit vent area. MOC image E10-02068, 196.05° W, 7.81° N, 4.62 m/pixel. (c) Linear summit vent area. MOC image E09-01208, 197.15° W, 16.68° N, 6.28 m/pixel. (d) Linear summit vent area. MOC image E11-04266, 197.57° W, 7.93° N, 4.63 m/pixel.

Table 1
Low shield morphometry

Location	Width (km)	Height (m)
0.01164° S/199.61993 (a)	70	85
4.74615° N/201.26920 (b)	57 × 72	57
7.00389° N/200.25969 (c)	71 × 75	101
7.87991° N/197.44573 (d)	95 × 71	113
7.05280° N/191.30598 (e)	124 × 102	98
6.60655° N/190.45357 (f)	73 × 41	50

Letters denote location in Fig. 4.

not well-defined in those images. Several MOC images illustrate the summit and flank morphologies of low shields (Figs. 5 and 6). The summit vent morphology varies from well-defined circular craters to linear vents to more subtle sags. The margins of the shields typically exhibit well-defined lava flows, but some of the summit areas do not.

Presumably the lava flows from the low shields were produced by lower effusion rates than at the fissures. Eruption rates might be have been similar to those observed in Hawaii (e.g., 50–90 m^3/sec) where the effusion rates are low enough to produce individual flows rather than large sheet flows. The large-scale sheet flows more characteristic of the Cerberus plains were probably produced by much higher rate eruptions. Keszthelyi et al. (2000) have discussed possible styles of eruption and emplacement for the Cerberus flows. Gregg and Sakimoto (2000) examined the flows in Marte Vallis and concluded that the effusion rates were of the order 10^3–10^4 m^3/sec, similar to the rates estimated by Keszthelyi et al. (2000). The difference in effusion rates would explain the morphologic differences between the two vent styles.

4. Fluvial sources

Two major sources of water that carve large channels are observed at the northwest end of Cerberus Fossae. The first (10.3° N, 203° W) occurs along the southern segment of the fossae, producing a narrow erosional trough—Athabasca Vallis (Figs. 1 and 7). A second source, proposed to be named Grjota' Vallis (Fig. 8), lies along the northern segment of the fossae at 15.6° N, 197.3° W. This channel system extends eastward into the knobby terrain and then southward possibly into the Cerberus plains. Both systems have morphologic characteristics typical of the channels produced by the catastrophic release of water (Carr, 1979; Baker, 1982; Baker et al., 1992; Baker and Milton, 1974; Baker and Kochel, 1979)—well-defined source areas, low sinuosity, longitudinal grooving of the channel floor, and scour around obstacles. The morphologic and hydrologic details of both areas has been discussed by Burr et al. (2002b, 2002a).

The water that carved Athabasca Vallis was released from two closely spaced sources about 23 km apart along the southern strand of the Cerberus Fossae (Figs. 7, 9). Here, the fossae are 35–40 km apart and trend N 67° W at an elevation of −2.5 km. The northwest source is 15–16-km long; the southeastern source is ∼ 12-km long. Troughs extend southwest from the source areas and converge ∼ 10 km downstream into a single channel ∼ 15-km wide and 100 m deep. Athabasca Vallis is traceable for 350 km to the southwest before it disappears beneath younger plains units near 6.6° N, 208° E (Fig. 12). Along its observed length, the average gradient is only ∼ 0.03°. The location and orientation of the channel is controlled by a southwest trending wrin-

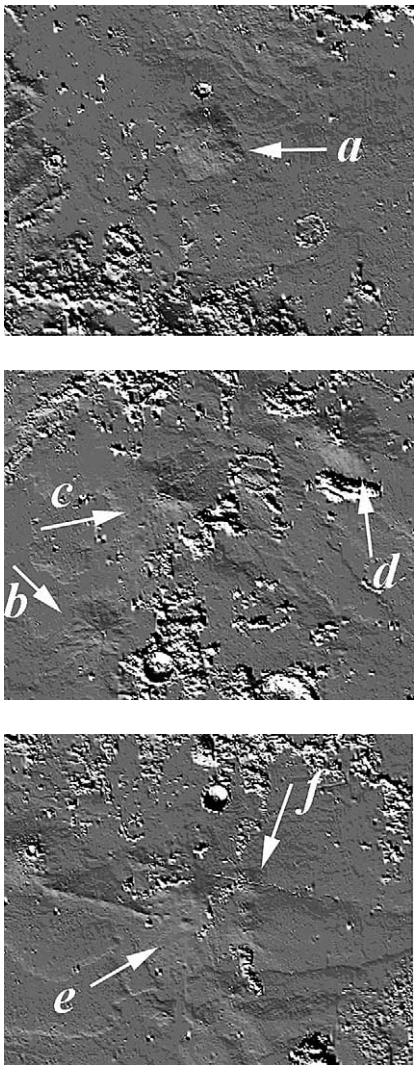

Fig. 4. Shaded MOLA relief images showing location and morphology of low shields. Letters correspond to entries in Table 1 and discussed in the text.

kle ridge on the adjacent older plains unit lying along the southeast side of the channel.

Nowicki and Christensen (2001) interpret TES data to indicate high (20–30%) rock abundance in Athabasca Vallis relative to the adjacent plains (< 10%). The roughness difference can be interpreted to indicate debris on a bare channel floor or a rough volcanic surface on the channel floor. In either case, the surface is rougher than the older plains units which may have thicker aeolian mantles than the channeled area.

North of the fossae and the source area for Athabasca Vallis, the plains units are older and have numerous small-diameter craters and dunes as seen in both Viking and MOC images. There is no evidence of fluvial erosion nor younger volcanic flows to the north of the fossae (e.g., M09-04594), indicating that the fossae are the source of the water for Athabasca.

Although albedo patterns in Viking images and low-resolution (250 m/pixel) MOC images hint at the presence of the source and channel, they are not definitive. However, high-resolution MOC images and MOLA topography clearly define the fluvial nature of the event. Trough and obstacle margins are terraced, the result of differential erosion of a layered unit, different flow levels, or separate fluvial events (Fig. 10a–c). Numerous craters, several kilometers in diameter on the channel floor that predate the flow, were eroded into tear-drop-shaped forms with the tapered end lying on the downstream side of the crater (Fig. 10b, c). The downstream tail could be an erosional remnant or depositional as Burr et al. (2002b) have suggested.

The channel floor in many locations is characterized by linear striae (Fig. 10d), referred to as longitudinal lineations by Burr et al. (2002a). Striae are 40–60 m apart and are topographic highs on an otherwise planar surface. In some locations, these striae appear to be composed of aligned hills having summit depressions. Much of the channel floor appears smooth, the striae and other morphologic features being buried. Material that buries the channel floor appears to be volcanic based on its morphology in MOC images, although the source region for the volcanics is unclear from the existing image coverage.

The morphology of aligned hills with summit depressions have been observed elsewhere in Cerberus and Amazonis. Lanagan et al. (2001) consider the morphology and dimensions of the hills with summit depressions to be similar to rootless volcanic cones in Iceland. The rootless Icelandic cones are formed when lava interacts with a wet substrate producing phreatic explosion deposits (e.g., Greeley and Fagents, 2001). Lanagan et al. interpret the presence of such features in the Cerberus area as forming when lava overrode ground with shallow water or ice. Burr et al. (2002a) propose an alternative explanation and interpret these features as due to catastrophic flooding. They suggest most are due to erosion, although they acknowledge that other processes (deposition around ice blocks, boulder trails) might be responsible for the variation in morphology (e.g., aligned hills with summit pits). More recently, Jaeger et al. (2003) suggest that these features could be exposed ring dikes. They note the morphologic and morphometric similarities between the features observed on the channel floors and features observed in the Channeled Scablands of Washington. The Scablands features are composed of steeply-dipping jointed basalt caused by sagging and foundering of a lava crust (McKee and Strandling, 1973), inflation pits or water-cooling induced jointing. Jaerger et al. favor the later two options. The inflation pit model, which I think is applicable, alleviates problems they identified with the sagging and foundering model and eliminates the need for active water circulation when the original volcanic plains were formed.

In addition to the primary Athabasca channel, narrow channels cut across the plains that lie along the southeast side of the channel (Fig. 10e). The largest of these channels begins at 9.111° N, 204.4° W at an elevation of −2620 m

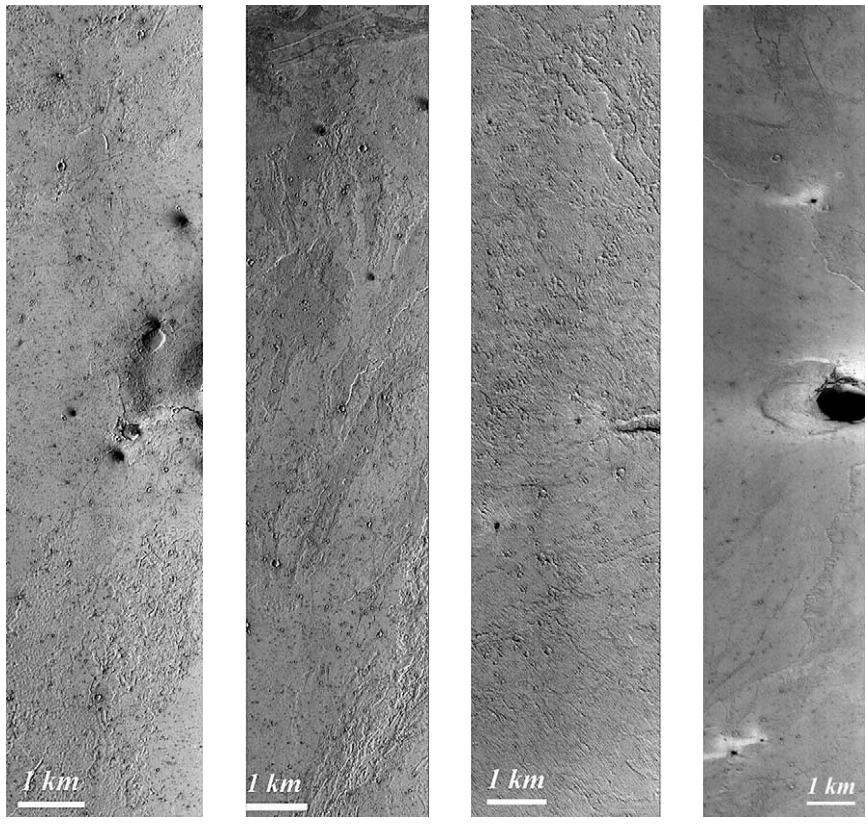

(a) (b) (c) (d)

Fig. 5. Morphology of low shields. (a) Western edge of the summit crater of low shield "a" (Fig. 4); the surrounding flank has a smooth texture. MOC image E04-02265, 199.72° W, 0.07° S, 4.38 m/pixel. (b) Northeast margin of the low shield of low shield "a" (Fig. 4) showing narrow lava flows extending down slope. MOC image E05-01258, 199.57° W, 0.08° S, 5.83 m/pixel. (c) Western margin of low shield "c" (Fig. 4) showing the edge of the summit vent and lava flows extending down the flank. MOC image E11-03181, 200.48° W, 7.21° N, 4.63 m/pixel. (d) Summit area of low shield "b" (Fig. 4) showing the summit vent area and flows extending down the flank. MOC image E10-04174, 201.33° W, 4.77° N, 3.06 m/pixel.

where it is about 450-m wide. About 2 km downstream it becomes a broader channel system ∼ 2.5-km wide. The channel can be followed for a total length of 60 km before it turns southwest and disappears beneath younger smooth plains at 8.024° N, 204.267° W at an elevation of −2660 m. Along the length of channel a few narrow (90–130 m) tributary valleys occur.

Both Athabasca Vallis and the smaller channels that erode the adjacent smooth plains disappear beneath younger widespread plains material (Fig. 11). The morphology, as revealed by both MOC (Fig. 12) and MOLA data, is similar to that of the central part of the Cerberus plains (Keszthelyi et al., 2000), suggesting these plains too are of volcanic origin. Thus, following the fluvial episode, it is suggested that a volcanic episode occurred burying the distal, low-elevation portions of the channels and locally filling the channel floors.

A second major fluvial source (referred to as Grjota' Vallis) lies along a northern segment of the Cerberus Fossae at 15.6° N, 197.3° W (Fig. 13) adjacent to the knobby terrain (Burr et al., 2002a). The source region for Grjota' Vallis extends ∼ 100 km along the fracture. Water released from this source carved a broad channel (60–100 km) with the flow diverging around obstacles and forming numerous scoured topographic highs. Elevations at the source area are −2.3 to −2.4 km and decrease by only 200–300 m along the well-defined length of the channel. Viking images of the region (Fig. 13) show no evidence of fluvial erosion. Subtle albedo/shading patterns are consistent with such erosion, but alone are not diagnostic.

MOC images (Fig. 14) show the morphology of the Grjota' channel floor is similar to that of Athabasca Vallis with a scoured surface. In the immediate vicinity of the fracture, scours is observed north and south of the fossae, but only to the north and northeast does the scour extend for a considerable distance. The channel has terraced margins and terracing downstream of craters and obstacles. Linear striae, some of which are composed of chains of hills with summit pits as in Athabasca, occur on the channel floor. Similar to Athabasca, much of the floor is smooth and the scour features have been buried by a younger smooth material.

In the Grjota' source region, the fossae trend N 75° W and are formed by several slightly offset, en echelon fractures that extend ∼ 360 km across volcanic plains and adjacent knobby terrain. The fractures are not observed to extend farther northwest toward Elysium Mons. To the southeast they disappear in the knobby terrain, although linear knobs pro-

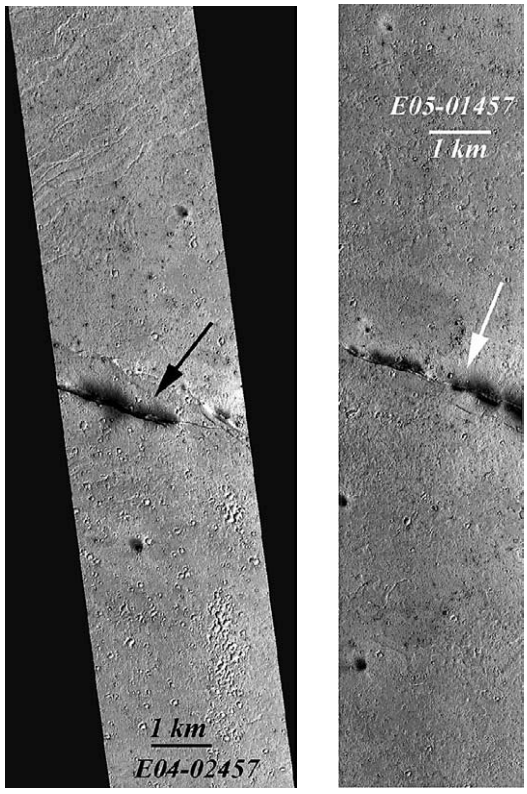

(a) (b)

Fig. 6. MOC images of low shield "d" (Fig. 4) 7.87991° N, 197.44573° W. This shield has a linear summit vent which is illustrated in the two images. (a) Well-defined lava flows are visible only in the upper part of image. MOC image E04-02457, 197.13° W, 7.79° N, 5.91 m/pixel. (b) Summit area showing a linear vent. However, little other volcanic detail is visible. MOC image E05-01457, 197.02° W, 8.05° N, 5.89 m/pixel.

trude through the plains material and there are narrow offset parallel fractures suggesting the structural trend continues to the southeast. Narrow grabens and fractures are scattered across much of the Tartarus Montes, cutting both the knobby terrain and intervening plains with similar strikes suggesting

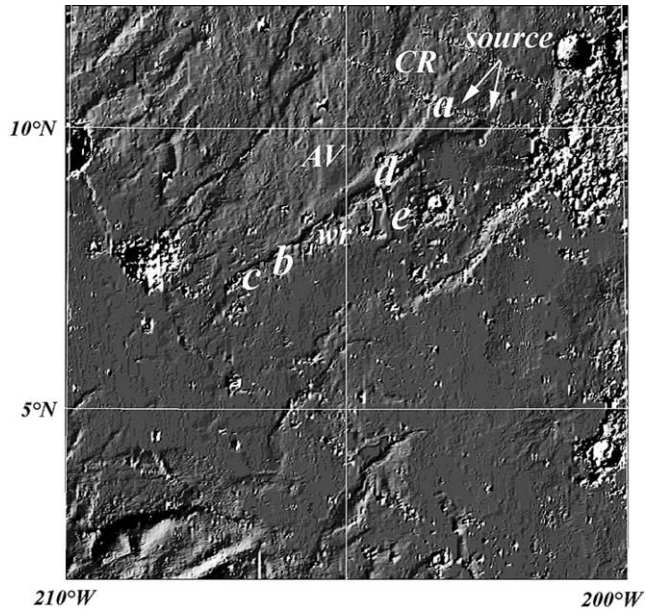

Fig. 7. MOLA topography of the Athabasca Vallis region along the western end of Cerberus Fossae at 10.3° N, 203° W. Note presence of southwest-trending wrinkle ridge ("wr") which controls the location of the trough. The locations of the MOC images in Fig. 10 are noted by letters (a)–(e).

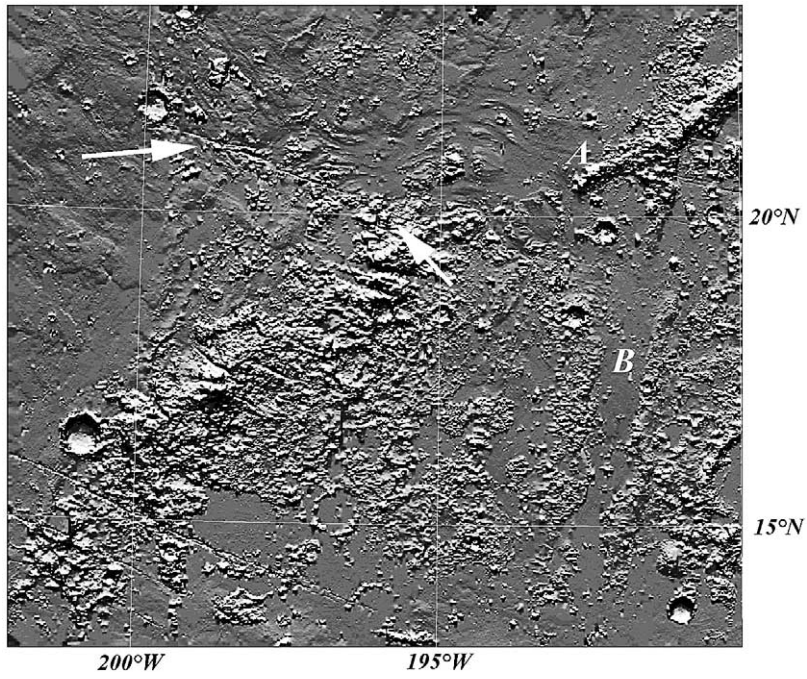

Fig. 8. MOLA shaded relief map of Grjota' Vallis region at 15.6° N, 197.3° W. Note the northeast-trending topographic ridge Tartarus Montes (A) in the knobby terrain. Illumination is from the north. Arrows denote extent of source along the fracture. South–southwest-trending trough is located at B.

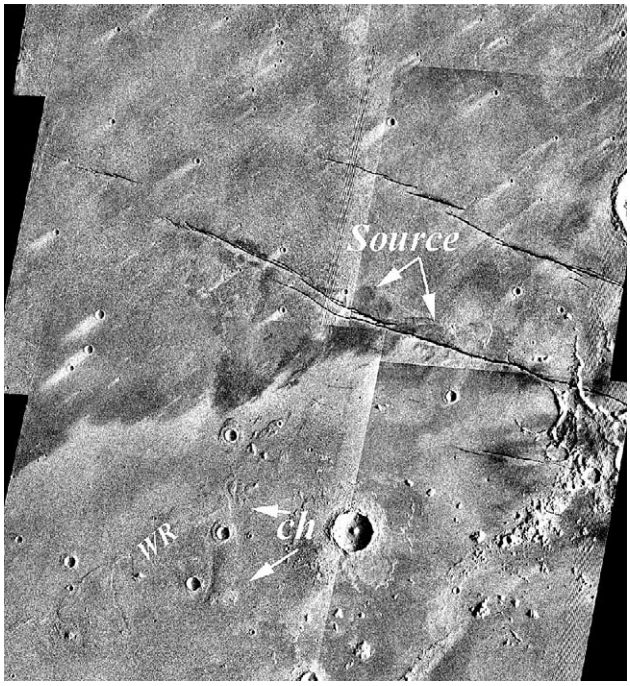

Fig. 9. Mosaic of Viking images (883A25-30) of Athabasca Vallis source region. Resolution 150 m/pixel. Note sources, older plains area with wrinkle ridge (WR) adjacent to the Vallis. Side channels denoted by ch.

a widespread tensional fracture system associated with Cerberus Fossae.

Grjota' Vallis begins with an east–northeast flow direction (N 58° E) and then turns southeast near longitude 195° W. Grjota' Vallis has a less well-defined shape compared with Athabasca Vallis. The Grjota' Vallis source occurs on a plains unit having scattered knobs. As the flow emerged from a long section of the fossae, it simply flowed across a broad region, around the knobs and craters. The resulting channel is broad, shallow and unconstrained, rather than deep and narrow as in Athabasca, where a wrinkle ridge confined the flow.

Near 15° N, 193° W the Vallis crosses the major northeast-trending (N 60° E) bedrock ridge of Tartarus Montes. Across a region ∼ 95-km wide, the ridge is interrupted and the channel passes through this topographic low and continues to the southeast. The Vallis can be traced another 80–100 km, but it is less well-defined than upstream. Near 14.8° N, 192.2° W, obvious flow morphology disappears into a south–southwest-trending (S 10° W) topographic trough.

This south–southwest trough parallels the regional topography and structure, extending ∼ 330 km southward to the Cerberus plains (Fig. 15a). MOC images show scour fea-

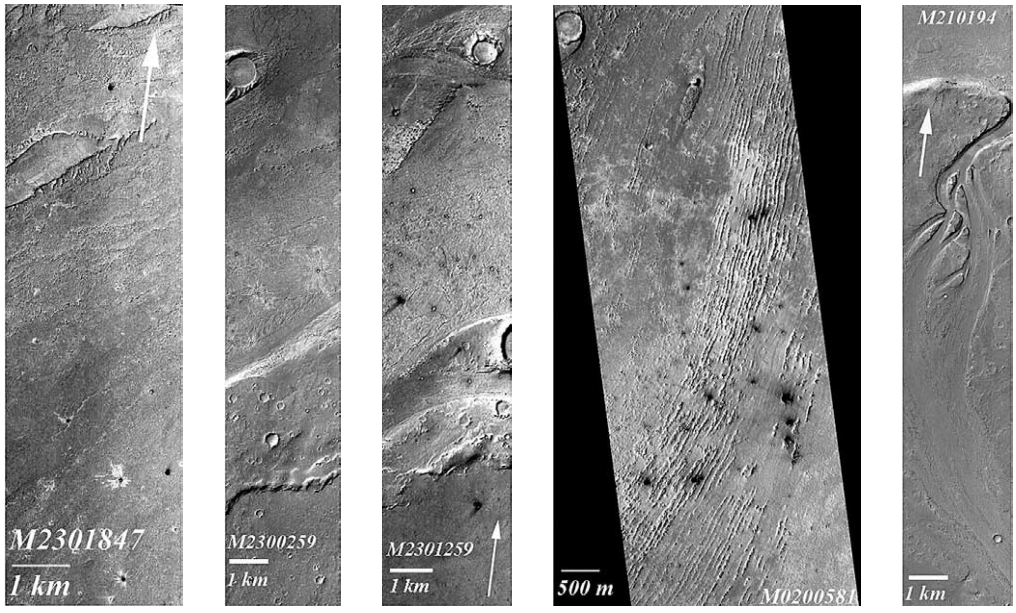

(a) (b) (c) (d) (e)

Fig. 10. MOC images of Athabasca Vallis and distributaries. (a) Channel floor immediately south of the Athabasca Vallis source. Channel floor is etched and scoured along the margins and locally buried with lava farther from the margins. Arrow indicates north, 5.89 m/pixel. Scene is 3.01-km wide. MOC image M23-01847, 203.45° W, 10.24° N, 5.89 m/pixel. (b) Southern margin of the channel and the southwest trending wrinkle ridge and older plains on the south, 5.87 m/pixel. Scene is about 3-km wide. Part of MOC image M23-00259, 206.24° W, 7.56° N, 5.87 m/pixel. (c) Southern margin of the channel and adjacent southwest-trending wrinkle ridge. The higher parts of the channel floor are clearly scoured and grooved, whereas the lower areas are covered with lava, 2.93 m/pixel. Scene is 3-km wide. Part of MOC image M23-01259, 206.71° W, 7.54° N, 2.93 m/pixel. (d) Channel floor showing linear striae 40–60 m apart. Many are composed of coalesced round hills with summit depressions. Scene is 3-km wide. Portion of MOC image M02-00581, 204.55° W, 9.26° N, 5.87 m/pixel. (e) Narrow channel cutting south from Athabasca Vallis across an older plains unit. Channel is 330 m wide at north end and broadens to 2.4 km at southern end. Scene width 2.91 km. Part of MOC image M21-01914, 206.05° W, 7.89° N, 4.40 m/pixel.

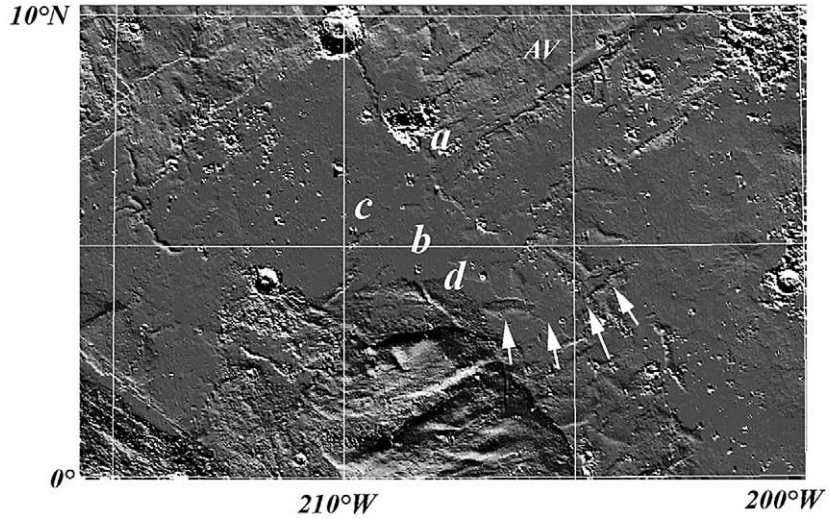

Fig. 11. Shaded relief image of the region at the south end of Athabasca Vallis showing the smooth plains that cover the distal end of the channel and embay the older ridged plains that lie along the southeast side of the channel. A trough occurs across the higher areas at the southern end of the plains (denoted by arrows) allows flow into the Cerberus plains. The location of the images in Fig. 12 are noted by letters.

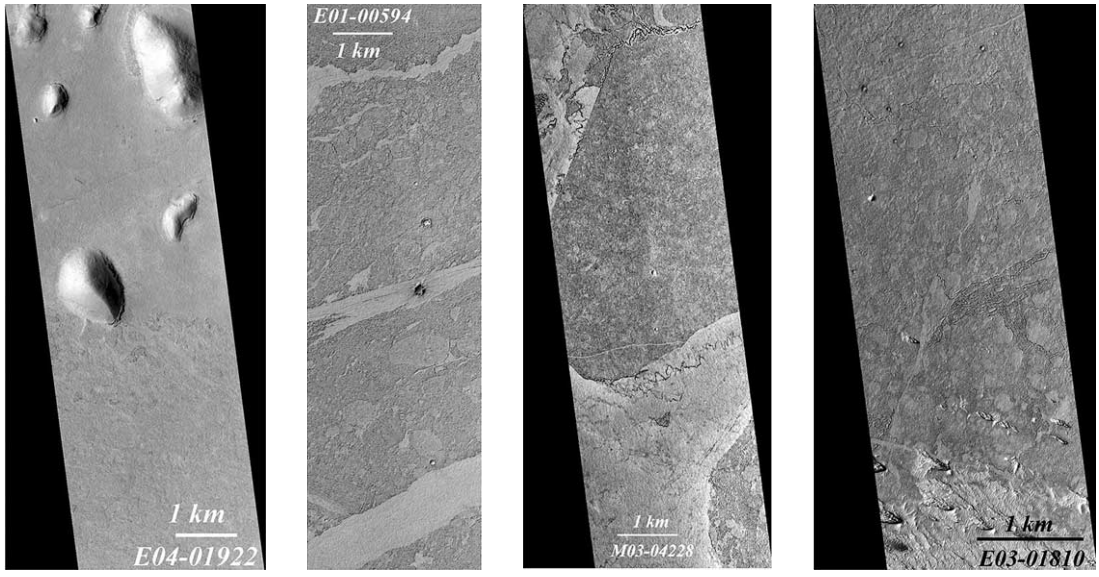

(a) (b) (c) (d)

Fig. 12. MOC images of the plains that cover the distal end of Athabasca Vallis. (a) Contact between the volcanic plains and the older plains with knobs. MOC image E04-01922, 207.85° W, 7.00° N, 5.90 m/pixel. (b) Central portion of the volcanic plains. MOC image E01-00594, 207.89° W, 5.06° N, 2.92 m/pixel. (c) Central portion of the volcanic plains. MOC image M03-04228, 209.89° W, 5.88° N, 2.91 m/pixel. (d) Southern margin of the volcanic plains showing the characteristic morphology and the presence of an overlying brighter material with dune-like morphology. This brighter southern unit is part of the Lower Member of the Medusae Fossae Formation. MOC image E03-01810, 208.07° W, 4.28° N, 2.92 m/pixel.

tures in a few places along the trough margins (Fig. 15b) indicating that fluvial erosion has occurred here and that the water flowed in a southward direction. However, most of the plains within the trough have a smooth surface, a younger unit presumably buries a more widespread eroded surface. The presence of flow fronts suggests the smooth plains are volcanic. This south–southwest trending trough provides a path for the water flowing through Grjota' Vallis to reach the Cerberus plains and ultimately Marte Vallis. Such a flow regime was suggested by Berman and Hartman (2002).

5. Valley system

In addition to the large channel systems of Athabasca and Grjota' noted above, an extensive valley network occurs on the plains south of Orcus Patera near 9.2° N, 184.8° W (Fig. 16) referred to here as Rahway Vallis. This system was briefly discussed by Head and Kreslavsky (2001) who noted that the channels were shallow and suggested they were V-shaped in MOLA data. Burr et al. (2002a) also mention it in their discussion of fluvial activity in the Cerberus

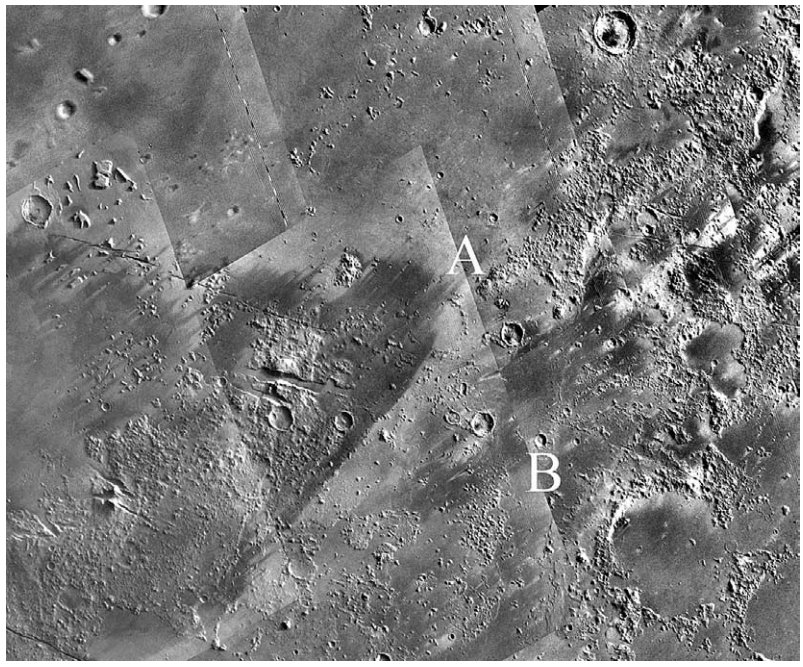

Fig. 13. Viking mosaic of the Grjota' Vallis source area, 1 km/pixel. Flow cuts through Tartarus Montes at A. South–southwest-trending trough is located at B.

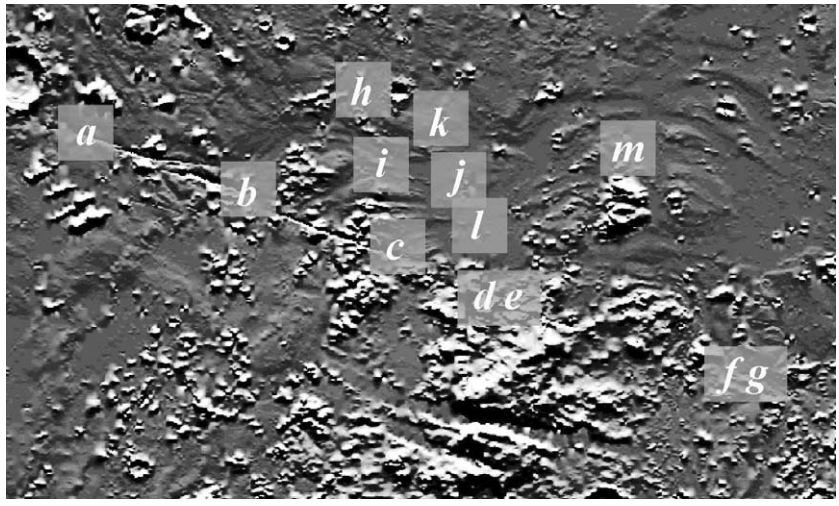

(a)

Fig. 14. (a) Index figure of Grjota' Vallis showing location of the high-resolution MOC figures at (b)–(m). (b) Northeast end of the fracture showing erosion and flow to the southwest, as opposed to the primary flow direction to the northeast. Part of MOC image E12-00531, resolution 6.26 m/pixel, 15.8° N, 199.45° W. (c) Portion of fracture showing erosion and steep cliff on upper part of fracture walls. Part of MOC image E04-00971, resolution 5.98 m/pixel, 16.40° N, 198.47° W. (d) Portion of fracture showing scour to the north. Part of MOC image E11-02496, resolution 6.26 m/pixel, 15.58° N, 196.86° W. (e) Narrow portion of fracture source area. Part of MOC image E12-00763, resolution 6.25 m/pixel, 15.53° N, 195.56° W. (f) Portion of fracture showing scoured and eroded surface to the north. Part of MOC image E02-02487, resolution 5.97 m/pixel, 15.49° N, 196.01° W. (g) Source along the fracture at its southeast end. Part of MOC image E10-03630, resolution 4.67 m/pixel, 14.64° N, 194.05° W. (h) Scour at southeast end of the fracture, flowing around obstacles. Note also the young apparently uneroded crack. Part of MOC image M04-03295, resolution. (i) Scour around obstacles on channel floor. Part of MOC image E09-01029, resolution 6.28 m/pixel, 16.68° N, 197.15° W. (j) Scour around obstacles on channel floor. Part of MOC image E11-02496, resolution 6.26 m/pixel, 15.58 N, 196.86 W. (k) Scour features on channel floor. Part of MOC image E05-00768, resolution 5.98 m/pixel, 7.4 m/pixel, 9.62° N, 182.96° W. (l) Scour features on channel floor. Part of MOC image E11-01240, resolution 6.26 m/pixel, 16.44° N, 196.09° W. (m) Streamlined island in the channel. Part of MOC image E02-02487, resolution 5.97 m/pixel, 5.97 m/pixel, 15.49° N, 196.01° W. (n) Streamlined island in the channel. Part of MOC images E11-04500, resolution 6.26 m/pixel, 16.15° N, 194.81° W.

region. Several of the valleys extend up to 450 km westward across the older plains unit that stands ∼ 10–20 m above the lava surface in Marte Vallis. The valleys predate the lavas of the Cerberus plains and Marte Vallis since they do not extend across the contact between the older plains and the lavas. The morphology and topography of the valleys indi-

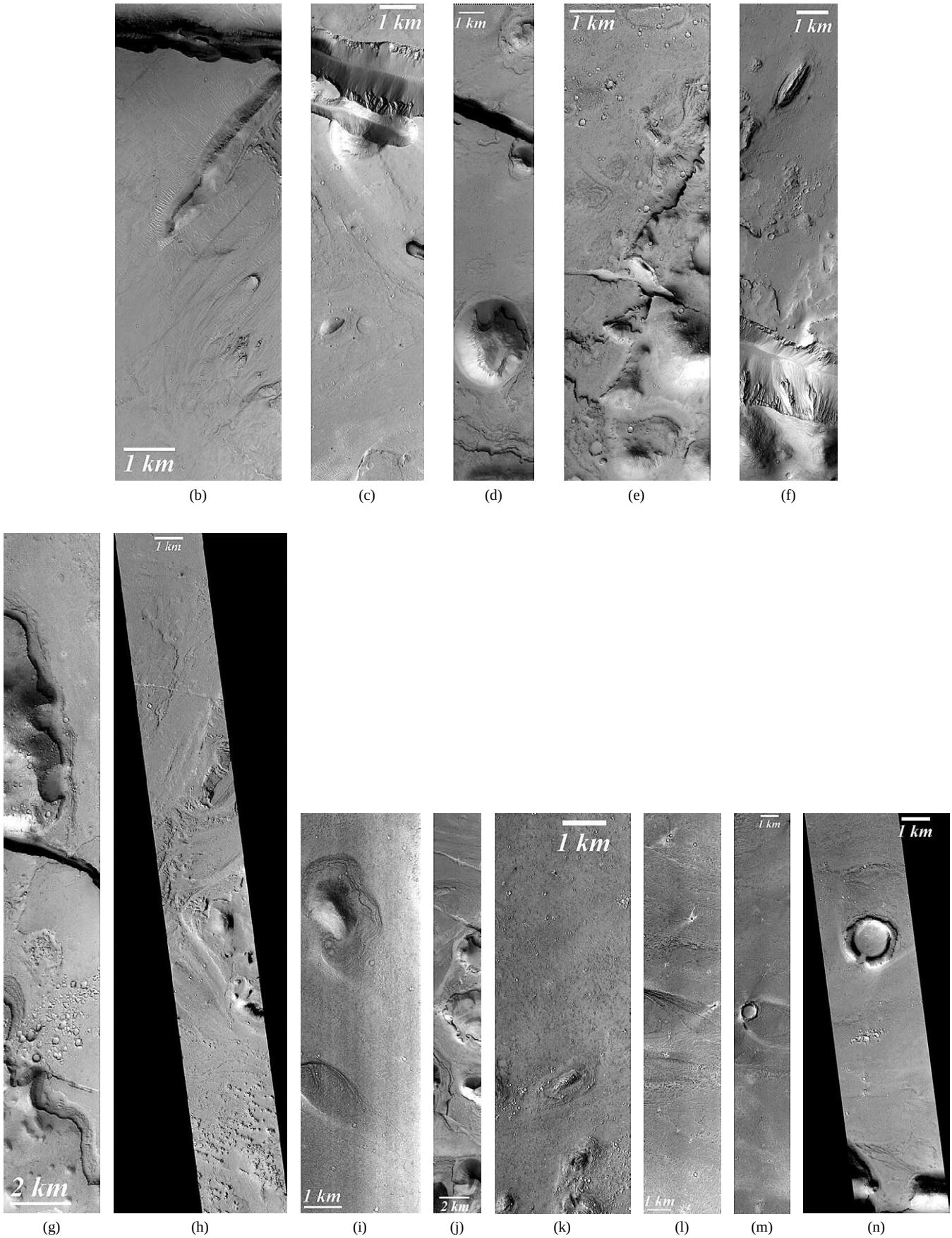

(b) (c) (d) (e) (f)

(g) (h) (i) (j) (k) (l) (m) (n)

Fig. 14. (Continued.)

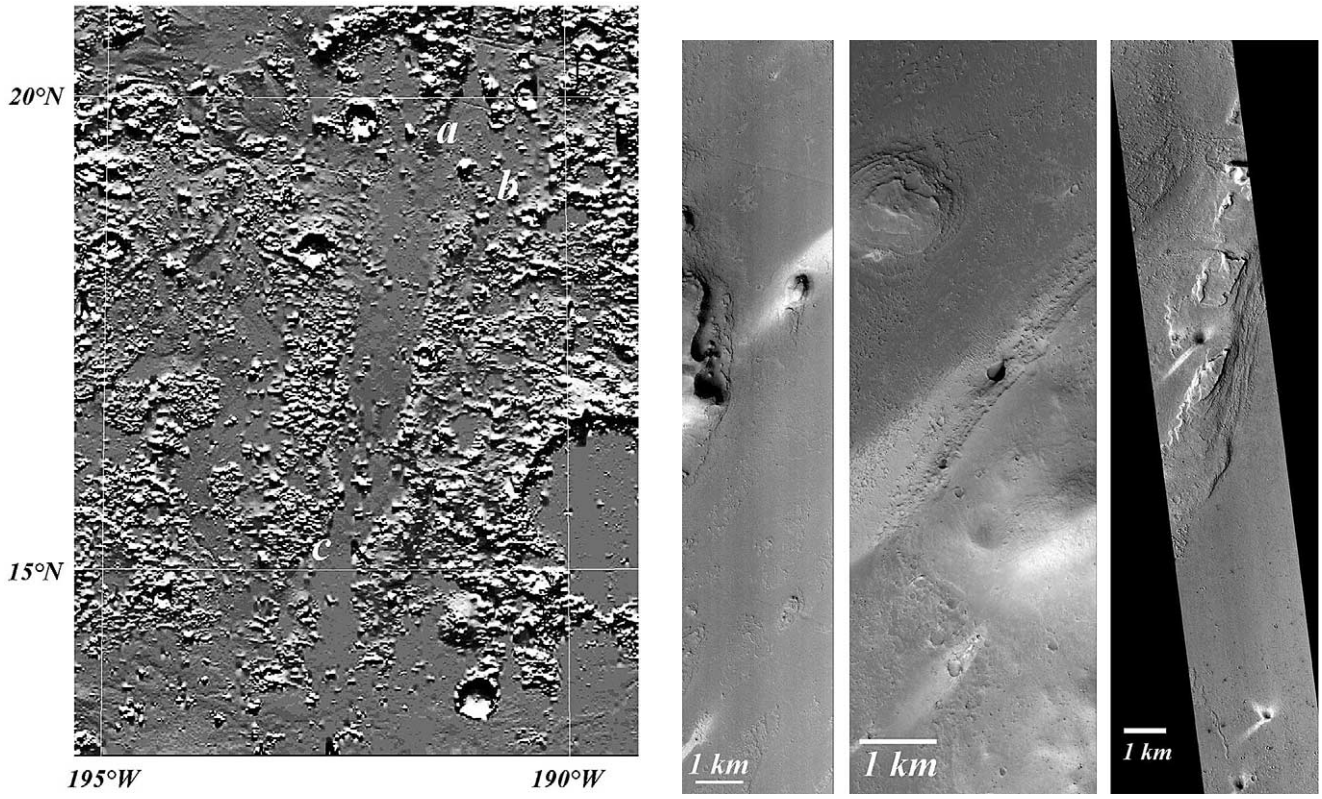

Fig. 15. South–southwest-trending through the knobby terrain connecting Grjota' Vallis with Cerberus plains. Letters (a)–(b) denote the location of MOC images in Fig. 15b. (a) MOLA relief showing trough in the knobby terrain. Trough is floored with younger plains material covering scoured surface, except locally along the margins. (b) Scoured surface along the western margin of the trough at its southern end. Channel floor covered with smooth material burying scoured surface. Scene width 3 km. Portion of MOC image M07-05670, 10.0° N, 192.8° W, 5.87 m/pixel.

cate that they drained into Marte Vallis before it was filled with lava.

Rahway Vallis has several major branches forming a well-defined dendritic pattern. Two of the branches begin at the Cerberus Fossae, which apparently was the source for some of the water that flowed through the valleys (Fig. 16). The most obvious source occurs at 6.794° N, 188.084° W (elevation −3012 m) and continues discontinuously along the fossae to the southeast for about 120 km. Two main valleys reach Marte Vallis at 9.574° N, 181.107° W (elevation −3117 m) and at 8.989° N, 183.745° W (elevation −3056 m). Between this second point and a location farther south (7.064° N, 185.399° W, elevation −3056 m) there are a number of small valleys carved into the edge of the older plains. These smaller valleys, which can be traced only a short distance across the older plains, are ∼ 20 m deep and 200–300 m wide where observed in MOC images (Fig. 17). MOC images show the channels to be filled. The channel filling material has a flat-topped central ridge (∼ 100 m wide) flanked by troughs ∼ 200 m wide—a much more complex morphology than the MOLA data alone would suggest (Head and Kreslavsky, 2001).

The erosional event that formed Rahway Vallis was of a different style than that which formed Athabasca or Grjota' Vallis. In addition to the sources along Cerberus Fossae, there was either a more widespread release of ground water or precipitation to account for the widespread distribution of the network. Water released from Cerberus Fosse must have been at a much lower rate than at Athabasca or Grjota' since a valley network system developed rather than a single large channel.

6. Discussion

MOC and MOLA data illustrate several fluvial and volcanic source areas in the region of Cerberus Fossae and on the Cerberus plains. The fractures of Cerberus Fossae have clearly controlled the location of water release as all of the principal fluvial sources are associated with the Fossae. It has also controlled the location of some of the volcanic eruptions. Several previous studies have suggested that the fossae were a source for water and volcanics (e.g., Plescia, 1990; McEwen et al., 1998; Berman et al., 2001); these suggestions are now well documented (see also Burr et al., 2002b, 2002a).

Cerberus Fossae is associated with radial elements of the Tharsis tectonic province (Hall et al., 1986; Plescia, 2001). The morphology and style of deformation indicate it is an extensional feature, although its en echelon nature may suggest

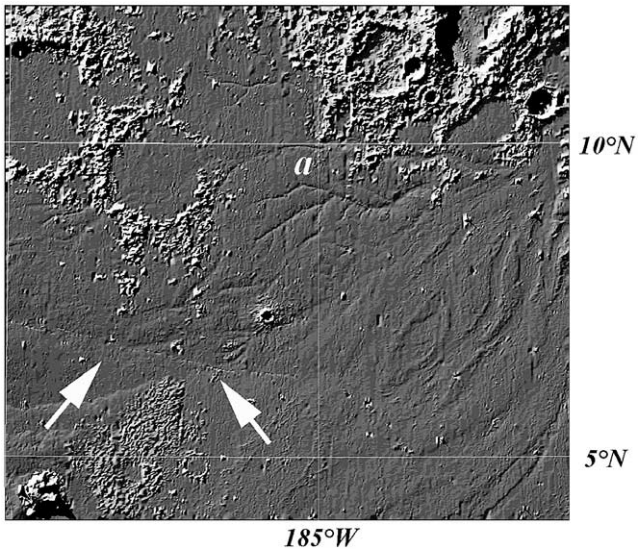

Fig. 16. MOLA relief of the Rahway Vallis network draining into Marte Vallis at 9.2° N, 184.8° W. The terminal end of the valleys are buried by the lava flows filling Marte Vallis. Arrows denote location of sources along Cerberus Fossae. The locations of the images in Fig. 17 are annotated on the map by the letter (a).

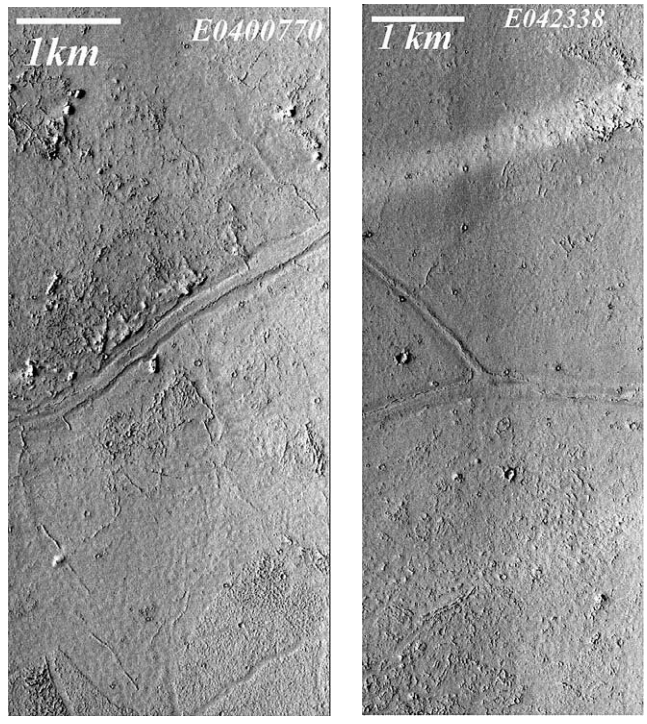

(a) (b)

Fig. 17. MOC images of the Rahway Vallis network near 9.2° N, 184.8° W. (a) The main valley trending northeast with a central ridge and flanking troughs. Portion of MOC images E04-00770, 184.94° W, 9.05° N, resolution 5.90 m/pixel. (b) Section of the main valley with morphology similar to that noted above and a tributary entering from the north. Portion of MOC image E04-02338, 184.78° W, 9.12 N, resolution 5.92 m/pixel.

a slight lateral component of displacement as well. Its great linear extent suggests it extends to a considerable depth. Although an open fracture would not extend very deep, the zone of weakness could feasibly extend through the crust. This subsurface zone of weakness could provide a conduit for magma from depth as well as for water from shallow subsurface aquifers. The occurrence of the water sources on the northwest and southeast ends of the fossae, and their absence elsewhere along the fracture, indicate that Cerberus Fossae itself alone does not control the release points for water. There must be specific isolated aquifers at depth that are penetrated at the points along the fossae when the channeling begins.

The specific subsurface reservoirs are impossible to identify. Source elevations for Athabasca (−2.5 km) and Grjota' Vallis (−2.3 to −2.4 km) are similar, suggesting that the water was released from the same aquifer at those two locations. Given the regional topography (higher to the west), that aquifer may extend beneath the Elysium rise. Such a geometry would provide a natural hydrostatic head and a large source region. The source area for the Rahway Vallis lies at an elevation of −3.0 km. The observation that water did not escape between the source areas for Athabasca and Grjota' Vallis and this part of fossae suggests that a separate aquifer was punctured at this point, or if volcanic heating is responsible a different shallow intrusion occurred there.

Linear fractures commonly act as conduits in terrestrial volcanic regimes for the ascent of magma to the surface (e.g., Kuntz et al., 2002; Luhr et al., 2001; Conway et al., 1997; Pinter, 1995). Wilson and Head (2002) have proposed that the linear grabens and fractures in Tharsis are associated with linear subsurface dikes. They note that such dikes could have fed the extensive flood basalt units. If such a dike(s) underlies the Cerberus Fossae, then it could be the source for the lavas of the Cerberus plains.

Linear fractures also appear to localize the release of water on Mars. Perhaps one of the most dramatic examples is Mangala Valles, which extends northward for hundreds of kilometers from a northeast-trending fracture of Memnonia Fossae (Zimbelman et al., 1992; Craddock and Greeley, 1994). Apparently, the fracture tapped a subsurface reservoir to release water onto the surface at catastrophic rates.

The presence of subsurface water reservoirs has long been suggested. Carr (1979, 2002) proposed a model in which high hydrostatic pressures develop within an aquifer trapped between a thickening cryosphere and impermeable basement rocks. Ultimately, the pressure exceeds the strength of the overlying crust and water is released spontaneously, or the cryosphere may be breached by faulting. Such a cryosphere, having variable depth depending upon latitude (extending to deeper depths at the pole) and time (extending to deeper depths with time), has been discussed by Clifford and Parker (2001 and references therein). At equatorial latitudes, Clifford and Parker (2001) suggest the cryosphere extends at present to depths of 2–5 km (water below those depths would be liquid and frozen at shallower depths). In the case of the release along Cerberus Fossae then, the fractures would have to penetrate several

kilometers to reach the liquid water. At these depths, the water should have significant hydrostatic pressure; the exact amount depending upon the details of the reservoir.

An alternative model to produce the water is melting due to volcanic intrusion. McKenzie and Nimmo (1999) propose dike intrusion as a mechanism to melt subsurface ice. Wilson and Head (2002) have argued that linear mafic dikes, which they believe underlie many of the grabens in the Tharsis and the Elysium regions, could produce significant heat that would melt the ground ice and release water onto the surface. They have proposed this as the mechanism for release of water to form Mangala Vallis and Mitchell et al. (2003) suggest this mechanism specifically for the Cerberus area. Under conditions when the melted water is confined by a surficial permafrost layer, pressures can increase and possibly exceed lithostatic pressure with a subsequent catastrophic release of water. Harrison and Grimm (2002) have modeled amount and timing of groundwater produced due to intrusion heating. Their calculations suggested that water can be produced over periods of up to 100,000 years. A concern with a dike-intrusion/heating model is why if water was melted along the length of the Cerberus Fossae, it only reached the surface in a few locations.

The release rates and mechanisms at Rahway Vallis would appear to be different from that at Athabasca and Grjota' Vallis. The latter two are clearly catastrophic flood features with volumes and discharge rates that carved enormous channels (Burr et al., 2002a, 2002b). At Rahway Vallis, valleys begin at the fossae and on the plains elsewhere in the region. The distribution of valley heads suggests that there may have been a shallow aquifer over a broad area which was releasing water onto the surface. Perhaps the valleys that begin at the fractures were fed by a locally higher flow rate; elsewhere sapping may have been important in valley formation (Baker, 1990; Carr, 1996).

Kanuth and Burt (2002) and Travis (2003) have examined the effects of brines on allowing for spring flow on the martian surface at low temperatures. Andersen et al. (2002) have documented low temperature (5.2° C) spring in the Canadian Arctic which flow year round at salinities of $\sim$ 10%. Thus, high water temperatures are not necessary for a spring to occur or persist. An alternative explanation for the valleys is that they were formed by rainfall (Plescia, 1993). If the valley networks formed during the early phases of eruption of the Cerberus lavas, sufficient water vapor might have been released to allow for local rainfall.

An important question with respect to Athabasca and Grjota' Vallis and Marte Vallis is whether they were active at the same time and possibly form an integrated system or whether they represent discrete events in space and time. The absolute timing of the volcanic and fluvial events is constrained by the ages of the surfaces that have been channeled and those that bury the channels. There are two approaches to using craters to define the ages: statistics of craters larger than 1 km from Viking images and statistics of craters in the tens to hundreds of meters diameter range from MOC and THEMIS images.

Counts using large-diameter craters have the advantage of producing ages that are insensitive to small-scale geologic processes, but the disadvantage of requiring large areas which can average local geologic processes. Small-diameter craters have the advantage that statistics can be compiled over small areas allowing for detailed geologic histories, but the disadvantage that small-scale, unimportant (?), geologic activity can more easily influence the cratering record. In addition, it is unclear if the actual production function of craters in this size range is accurately understood. McEwen et al. (2003) have shown that the Cerberus Plains have an extensive field of secondary craters caused by a 10 km crater at 7.76° N, 194.054° W. These secondary craters would be spatially limited and significantly affect the counts of small diameter craters by adding large numbers of craters at an instant in time and possibly with a size-frequency distribution different from that of the production population.

Burr et al. (2002a) have considered the question of relative timing of the fluvial events using counts derived from MOC images. They conclude the channels are not temporally related citing topographic and age constraints. Their MOC counts are interpreted to indicate ages (using the chronology of Hartmann, 1999) of 2–8 Ma for Athabasca Vallis, 10–40 Ma for Grjota' Vallis, and 10–100 Ma for Marte Vallis. Based on these apparently disparate ages, they conclude that each of the systems was active at a different period in time and that they are not interrelated. They do suggest that the presence of a widespread mantling (e.g., Medusae Fossae Formation) would affect the cratering ages, possibly masking the true formation ages and producing exposure ages rather than formation ages. Berman et al. (2001), Hartmann and Berman (2000), and Burr et al. (2002a) have taken a similar approach and compiled crater statistics from MOC images. They suggested absolute ages for these events in the range of 10 to 100 Ma, although they show maps suggesting they are related.

Table 2 lists the crater frequencies derived from Viking images for several major stratigraphic surfaces. The plains that were eroded by the fluvial episode(s) are the volcanic plains of the southeastern flank of Elysium Mons and the ridged plains of Arcadia Planitia. These surfaces have ages of Late Hesperian to Early Amazonian (based on the chronology of Tanaka (1986)). The channel floors themselves have too small an area and have been resurfaced in part by later volcanism to provide meaningful crater statistics (at diameters $>$ 1 km) of their formation age. However, two overlying post-erosion plains units provide minimum age limits for the fluvial activity and the age of the regional volcanism. The plains at the end of the Athabasca Vallis have an age of Late Amazonian; the volcanic Cerberus plains are also of Late Amazonian age and, as noted above, are the youngest large-scale volcanic surface on the planet. Crater counts at the kilometer scale (Table 2) only weakly constrain the events in absolute time: volcanism at about 144 Ma and

Table 2
Crater counts for stratigraphic bounding surfaces

Region	Viking image	Number of craters $\geqslant D/10^6$ km^2					
		1 km	2 km	5 km	10 km	N	Area (km^2)
Cerberus plains	672A61, 66-65	89 ± 15	23 ± 8	5 ± 4	3 ± 3	11	408,415
Smooth plains at end of Athabasca Vallis	383S10,12,42	87 ± 33	38 ± 22	16 ± 4		77	81,679
Plains cut by Grjota' Vallis	220A8-13,16,18	1211 ± 143	372 ± 79	160 ± 52	31 ± 22	360	59,671
Plains at NW end of Cerberus Fossae	883A27-29	953 ± 110	422 ± 74	38 ± 22	22 ± 17		
Ridged plains	545A6,8,10,13,27,29	1670 ± 110	462 ± 58	(85 ± 25)	(23 ± 13)	559	138,192
Ridged plains	54530,32,51,53,54	2166 ± 161	443 ± 73	(54 ± 26)	(11 ± 12)	444	83,673
Plains cut by Grjota' Vallis	672A81,84	(3197 ± 128)	(693 ± 59)	102 ± 23	20 ± 10	94	196,485

N = number of craters counted. Area = counting area in km^2.

fluvial erosion between 144 Ma (the age of the overlying uneroded surface) and about 1700 Ma (the age of the eroded surface).

Burr et al. (2002a, 2002b) have argued for repeated fluvial and volcanic events associated with the channel systems and Cerberus Fossae. I have not observed any area in which stratigraphic units can be observed that document repeated fluvial and volcanic events in the same location. From my observations an original, older volcanic surface was eroded by a fluvial event(s) and that surface was then locally covered with a smooth plains unit. That younger smooth plains unit has morphologic characteristics that indicate it is of volcanic origin. These observations do not constrain the timing, only that in a given location there was a fluvial event and a later volcanic event.

Some sections of the fossae have a very fresh appearance, locally appear uneroded, and the scour features are locally faulted. Burr et al. (2002a) suggest a scenario for the pristine appearance of the fossae involving multiple events of water release from the fossae and flooding down slope, eruption of lavas along the fossae filling the fossae and covering the downstream channel floor, and then tectonic reactivation of the fossae to form a new fracture. While such a scenario does account for the morphology, a simpler explanation is equally viable. The edges of the fossae are, in part, scoured and do show evidence of erosion indicating they are not completely buried by lavas. Continuous calving of the wall, possibly due to continued tectonism, could produce the fresh appearance.

The next question is the extent to which Athabasca, Grjota', Rahway, and Marte Vallis are part of an integrated system, which in effect implies they are coeval. The channel forms of Marte Vallis indicate extensive erosion and a significant source. Athabasca and Grjota' Vallis could have provided the water to form the Marte Vallis channels. It does, however, imply a fluvial system that exceeds 2500 km in total length. Berman and Hartman (2002) have proposed such an integrated system in schematic form suggesting the flow from Grjota' Vallis went south toward Athabasca and also east and then south into the trough south of Tartarus Montes and then in the Cerberus plains as noted above.

The ultimate sink of the water released from Athabasca Vallis may have been to flow across the Cerberus plains, through Marte Vallis and into Amazonis Planitia. MOLA topography reveals a narrow east-trending trough to connect the basin at the distal end of Athabasca Vallis with the Cerberus plains. The trough (3.873° N, 206.673° W to 4.704° N, 203.597° W) is $\sim$ 200-km long cutting through a piece of ridged plains (Fig. 11). Water may have ponded behind this topographic high, carved an exit channel and drained into Cerberus plains. The drainage system of Rahway Vallis could have added to the flow, but it is of insufficient magnitude to have produced enough water to carve the channel system of Marte Vallis. In addition to the exposed sources, there may have been additional sources of water that are now buried by later lavas.

Burr et al. (2002a) suggest that the source area for Marte Vallis may have been the eastern-most end of Cerberus Fossae. The fossae clearly extend beneath the lavas of Marte Vallis as indicated by the subtle topographic expression noted above. Given that the fossae have acted as a conduit for water release elsewhere along its length, this part of the fossae could well have been a source.

The simplest geologic model for the fluvial and volcanic events, would be that fracturing along the northwest end of Cerberus Fossae released water from a pressurized subsurface aquifer forming Athabasca and Grjota' Vallis during essentially a single geologic event. An alternative model is that increasing pressure of the aquifer simply took advantage of a preexisting zone of weakness (the fossae) and broke out with no associated tectonism. In either case, flow would have continued until the aquifer was drained or until it resealed itself by freezing. A single event in time eliminates the requirement of recharging the aquifer or postulating repeated heating of an aquifer and melting to produce water. The relative timing of the events at the northwest and southeast end is less well-constrained. At the southeast end of the fossae the fluvial activity clearly predates the volcanism as the distal ends of Rahway Vallis are buried by lavas. Subsequent to the fluvial event, volcanics were erupted across the Cerberus plains from vents localized along Cerberus Fossae and from other vents scattered across the region.

Obvious pyroclastic deposits are not observed on the Cerberus plains. Widespread mantling material and the small conical hills with summit depressions (Lanagan et al., 2001) may represent local pyroclastic deposits. But the absence of large volumes of well-defined pyroclastic material would

argue against the fluvial and volcanic events being coeval. Given the volumes of water and volcanics, substantial pyroclastic deposits would be expected, particularly near the vents and release points along the Cerberus Fossae if both water and lava were being released from the same conduit at the same time.

Regardless of whether the absolute ages are in the range of hundred or tens of millions of years, the fluvial and volcanic events of the Cerberus region are among the youngest major geologic events on the planet. The Cerberus plains are only lightly cratered as are the channel floors of Marte, Athabasca, and Grjota' Vallis. The geology of the region indicates that both catastrophic fluvial events and major volcanic events have occurred in the recent geologic past and presumably could happen again. More about the faults.

Acknowledgments

The careful and thoughtful reviews of the manuscript by Jeffrey Johnson, Lisa Gaddis, Alfred McEwen, and a mysterious reviewer are greatly appreciated. Their comments and attention to the manuscript aided significantly in its revision. I also thank Derrick Hirsch whose editorial review significantly improved the manuscript. This research was supported by NASAs Planetary Geology and Geophysics Program.

References

Andersen, D.T., Pollard, W.H., McKay, C.P., Heldman, J., 2002. Cold springs in permafrost on Earth and Mars. J. Geophys. Res. 107. 10.1029/2000JE001436.

Baker, V., 1982. The Channels of Mars. University of Texas Press, Austin.

Baker, V., 1990. Spring sapping and valley network development. Geol. Soc. Amer. Spec. Paper 252, 235–265.

Baker, V., Milton, D., 1974. Erosion by catastrophic floods on Mars and Earth. Icarus 23, 27–41.

Baker, V.R., Carr, M.H., Gulick, V.C., Williams, C.R., Marley, M.S., 1992. Channels and valley networks. In: Kiefer, H.H., Jakosky, B.M., Snyder, C.W., Matthews, M.S. (Eds.), Mars. University of Arizona Press, Tucson, pp. 493–522.

Baker, V.R., Kochel, C., 1979. Martian channel morphology: Maja and Kasei Vallis. J. Geophys. Res. 84, 7961–7983.

Berman, D.C., Hartmann, W.K., Burr, D.M., 2001. Marte Vallis and the Cerberus plains; evidence of young water flow on Mars. Lunar Planet. Sci. 32. Abstract 1732.

Berman, D.C., Hartman, W.K., 2002. Recent fluvial, volcanic and tectonic activity on the Cerberus plains of Mars. Icarus 159, 1–17.

Burr, D.M., Grier, J.A., McEwen, A.S., Keszthelyi, L.P., 2002a. Repeated aqueous flooding from the Cerberus Fossae: evidence for very recent extant, deep groundwater on Mars. Icarus 159, 53–73.

Burr, D.M., McEwen, A.S., Sakimoto, S.E.H., 2002b. Recent aqueous floods from the Cerberus Fossae, Mars. Geophys. Res. Lett. 29. 10.1029/200GL013345.

Carr, M.H., 1979. Formation of martian flood features by release of water from confined aquifers. J. Geophys. Res. 84, 2995–3007.

Carr, M.H., 1996. Water on Mars. Oxford Univ. Press, New York. 229 p.

Carr, M.H., 2002. Elevations of water-worn features on Mars: implications for circulation of groundwater. J. Geophys. Res, 107.

Clifford, S., Parker, T., 2001. The evolution of the martian hydrosphere: implications for the fate of a primordial ocean and the current state of the northern plains. Icarus 154, 40–79.

Conway, F.M., Ferrill, D.A., Hall, C.M., Stamatakos, J.S., Connor, C.B., Halliday, A.N., Condit, C., 1997. Timing of basaltic volcanism along the Mesa Butte Fault in the San Francisco Volcanic Field, Arizona from $^{40}Ar/^{39}Ar$ dates: implications for longevity of cinder cone alignments. J. Geophys. Res. 102, 815–824.

Craddock, R.A., Greeley, R., 1994. Geologic map of the MTM-20147 Quadrangle, Mangala Vallis region of Mars. US Geological Survey Misc. Invest. Ser. Map I-2310.

Greeley, R., 1982. The Snake River Plain, Idaho: representative of a new category of volcanism. J. Geophys. Res. 87, 2705–2715.

Greeley, R., Fagents, S.A., 2001. Icelandic pseudocraters as analogs to some volcanic cones on Mars. J. Geophys. Res. 106, 20,527–20,546.

Greeley, R., Guest, J.E., 1987. Geologic map of the eastern equatorial region of Mars, 1:15,000,000 scale. US Geological Survey Misc. Invest. Ser. Map I-1802B.

Gregg, T.K.P., Sakimoto, S.E.H., 2000. Marte Vallis lava channel flow rates and rheology from MOC and MOLA data. Lunar Planet. Sci. 31. Abstract 1758.

Hall, J.L., Solomon, S.C., Head, J.W., 1986. Elysium region Mars: tests of lithospheric loading models for the formation of tectonic features. J. Geophys. Res. 91, 11,377–11,392.

Harmon, J.K., Arvidson, R.E., Guiness, E., Campbell, B.A., Slade, M.A., 1999. Mars mapping with delay-Doppler radar. J. Geophys. Res. 104, 14,065–14,089.

Harrison, K.P., Grimm, R.E., 2002. Controls on martian hydrothermal systems: application to valley network and magnetic anomaly formation. J. Geophys. Res. 107. 10.1029/2001JW001616.

Hartmann, W.K., 1999. Martian cratering VI. Crater count isochrons and evidence for recent volcanism from Mars Global Surveyor. Meteor. Planet. Sci. 34, 159–166.

Hartmann, W.K., Berman, D.C., 2000. Elysium Planitia lava flows: crater count chronology and geological implications. J. Geophys. Res. 105, 15,011–15,025.

Head, J.W., Kreslavsky, M.A., 2001. Plains in eastern Elysium Planitia, Mars: topographic evidence for aqueous channels and lava flows. Lunar Planet. Sci. 32. Abstract 1002.

Jaeger, W.L., Keszthelyi, L.P., Burr, D.M., McEwen, A.S., Baker, V.R., Miyamoto, H., Beyer, R.A., 2003. Ring dike structures in the channeled scablands as analogs for circular features in Athabasca Valles, Mars. Lunar Planet. Sci. 34. Abstract 2045.

Keszthelyi, L., McEwen, A.S., Thordarson, T., 2000. Terrestrial analogs and thermal models for martian flood lavas. J. Geophys. Res. 105, 15,027–15,049.

Kanuth, L.P., Burt, D.M., 2002. Eutectic brines on Mars: origin and possible relation to young seepage features. Icarus 158, 267–271.

Kuntz, M.A., Anderson, S.R., Champion, D.E., Lanphere, M.A., Grunwald, D.J., 2002. Tension cracks, eruptive fissures, dikes, and faults related to late Pleistocene–Holocene basaltic volcanism and implications for the distribution of hydraulic conductivity in the eastern Snake River Plain, Idaho. Geol. Soc. Amer. Spec. Paper 353, 111–133.

Lanagan, P.D., McEwen, A.S., Keszthelyi, L.P., Thordarson, T., 2001. Rootless cones on Mars indicating the presence of shallow equatorial ground ice in recent times. Geophys. Res. Lett. 28, 2365–2367.

Luhr, J.F., Henry, C.F., Housh, T.B., Aranda-Gomez, J.J., MacIntosh, W.C., 2001. Early extension and associated mafic alkalic volcanism from the southern Basin and Range Province, geology and petrology of the Rodeo and Nazas volcanic fields, Durango, Mexico. Geol. Soc. Amer. Bull. 113, 760–773.

McEwen, A., Turtle, E., Burr, D., Milazzo, M., Lanagan, P., Christensen, P., Boyce, J., The THEMIS Science Team, 2003. Discovery of a large rayed crater on Mars: implications for recent volcanic and fluvial activity and the origin of martian meteorites. Lunar Planet. Sci. 34. Abstract 2040.

McEwen, A.S., 1999. Flood lavas on Mars. Geol. Soc. Amer. Abstr. Prog. 31, 131.

McEwen, A.S., Edgett, K.S., Malin, M.C., Keszthelyi, L., Lanagan, P., 1998. Mars global surveyor camera tests the Elysium basin controversy; it's lava, not lake sediments. Geol. Soc. Amer. Abstr. Prog. 30, 402.

McKee, B., Strandling, D., 1973. The sag flowout: a newly described volcanic structure. Geol. Soc. Amer. Bull. 81, 2035–2044.

McKenzie, D., Nimmo, F., 1999. The generation of martian floods by the melting of ground ice above dykes. Nature 397, 231–233.

Mitchell, K.L., Wilson, L., Head, J.W., 2003. Dike emplacement as a mechanism for generation of massive water floods at Cerberus Fossae, Mars. Lunar Planet. Sci. 35. Abstract 1332.

Nowicki, S., Christensen, P., 2001. A new view of the surface of Mars: high-resolution rock abundances from MGS TES. Eos Trans. AGU 82, F723.

Pinter, N., 1995. Faulting on the volcanic tableland, Owens Valley, CA. J. Geology 103, 73–83.

Plescia, J.B., 1990. Recent flood lavas in the Elysium region of Mars. Icarus 88, 465–490.

Plescia, J.B., 1993. An assessment of volatile release from recent volcanism in Elysium, Mars. Icarus 104, 20–32.

Plescia, J.B., 2001. Elysium Region Tectonics. Lunar Planet. Sci. 32. Abstract 1088.

Sakimoto, S.E.H., Gregg, T.K.P., Hughes, S.S., Chadwick, J., 2003. Martian plains volcanism in Syria Planum and Tempe Mareotis as analogs to the eastern Snake River Plains Idaho: similarities and possible petrologic contributions to topography. Lunar Planet. Sci. 35. Abstract 1740.

Scott, D.H., Chapman, M.G., 1995. Geologic and topographic maps of the Elysium paleolake basin, Mars. US Geological Survey Misc. Invest. Ser. Map I-2397.

Tanaka, K.L., 1986. Stratigraphy of Mars. J. Geophys. Res. 91, E139–E158.

Tanaka, K.L., Chapman, M.G., Scott, D.H., 1992. Geologic map of the Elysium region of Mars. US Geological Survey Misc. Invest. Ser. Map I-2147.

Thorarinsson, S., 1970. The Lakaggar eruption of 1783. Bull. Volc 33, 910–929.

Thordarson, T., Self, S., 1993. The Laki (Skaftar Fires) and Grimsvotn eruptions in 1783–1785. Bull Volc. 55, 233–263.

Travis, B.J., 2003. On the impact of brines on hydrothermal circulation below martian permafrost. Lunar Planet. Sci. 34. Abstract 2063.

Wilson, L., Head, J.W., 2002. Tharsis-radial graben systems as the surface manifestations of plume-related dike intrusion complexes: models and implications. J. Geophys. Res. 107. 10.1029/2001JE001593.

Zimbelman, J.R., Craddock, R.A., Greeley, R., Kuzmin, R.O., 1992. Volatile history of Mangala Vallis, Mars. J. Geophys. Res. 97, 18,309–18,317.